*Journal of Inclusion Phenomena and Molecular Recognition in Chemistry* **20:** 211–232, 1995.



# Structural Patterns in Clathrates and Crystalline Complexes of Zinc-Tetra(4-Chlorophenyl)Porphyrin and Zinc-Tetra(4-Fluorophenyl)Porphyrin

HELENA KRUPITSKY, ZAFRA STEIN and ISRAEL GOLDBERG*
*School of Chemistry, Sackler Faculty of Exact Sciences, Tel-Aviv University, 69978 Ramat-Aviv, Israel.*

(Received: 25 July 1994; in final form: 17 January 1995)

**Abstract.** Twelve new crystalline materials based on zinc-tetra(4-chlorophenyl)porphyrin (8 compounds) and zinc-tetra(4-fluorophenyl)porphyrin (4 compounds) building blocks have been prepared and characterized by X-ray diffraction analysis. Several different modes of guest solvent incorporation into the porphyrin lattice, including enclathration (of solvents of low polarity) and complex formation (with strong Lewis bases), and of intermolecular organization have been detected. Unique interporphyrin architectures, affected by directional Cl···Cl interactions, characterize most of the known solid structures of the chlorosubstituted materials. A small number of the latter, as well as the fluorosubstituted derivatives, exhibit interporphyrin arrangements of the type which are commonly observed in the clathrates of unsubstituted tetraphenylmetalloporphyrins. The pore structure of these compounds is affected to a large extent by the nature of the incorporated solvate and, consequently, the degree of coordination of the metal center. In crystals of four-coordinate porphyrins the solvent guest components are usually incorporated into channel-type cavities formed between columns and layers of densely stacked hosts. In five-coordinate and six-coordinate materials the guest sites coincide with the axial coordination sites of the porphyrin metal atoms. The latter structures reveal a tight fit between adjacent layers of the complexed entities, the axial ligands of one layer being incorporated into localized interporphyrin cavities of another layer. Dipolar forces play also an important role in the interporphyrin organization.

**Key words.** Zinc-tetra(4-chlorophenyl)porphyrin, zinc-tetra(4-fluorophenyl)porphyrin, crystalline complexes of, aggregation modes of.

**Supplementary Data** relating to this article have been deposited with the British Library as supplementary publication No. SUP 82183 (97 pages).

## 1. Introduction

Crystalline aggregation of tetraphenylporphyrin (TPP) and tetraphenylmetalloporphyrin (M-TPP) was found to be dominated primarily by the molecular shape of these compounds. The structural systematics of such materials has been elucidated in a series of recent publications, revealing conservation of the porphyrin host structure in over 200 lattice clathrates based on the TPP building blocks [1–4]. The bulky and pseudo-rigid TPP framework, with four aryl rings nearly perpendicular

* Author for correspondence.

to the porphyrin core, can pack densely only in two dimensions, thus yielding in most cases hollow architectures (interporphyrin cavities and channels) in the condensed crystalline state. Correspondingly, crystallization of the TPP materials is often associated with incorporation of a 'guest' component into the crystal lattice, via either simple enclathration or metal coordination. The resulting solids represent a novel type of microporous materials ('porphyrin sponges'), and can be used for a variety of applications, such as isolation, separation and controlled release of molecular moieties.

Functionalization of the rigid porphyrin molecular framework with polarized aryl groups can be used to develop simple chemical models of self-assembly via weak intermolecular forces. In this context, we have indicated recently that it is possible to induce specific modes of interporphyrin organization by introducing polar sensor groups into the molecular framework [5,6]. For example, the tetra-(4-hydroxyphenyl)porphyrin moiety [4(OH)TPP] can form characteristic two-dimensional polymeric chains and three-dimensional networks via intermolecular hydrogen-bond linkages between the peripheral functions. Initial examination of crystalline structures based on the tetra(4-chlorophenyl)metalloporphyrin entity showed similar modes of intermolecular organization, suggesting that direct Cl···Cl interactions, along with dipolar interactions between chlorophenyl groups, are also significant in determining the interporphyrin architecture [5]. Effective formation of one-dimensional and three-dimensional coordination polymers based on metallated tetra(4-pyridyl)porphyrin, and directed by pyridyl-to-metal ligation has also been previously demonstrated [6].

The current study focuses further on the halogen-substituted tetraphenylmetalloporphyrin building blocks. We report here on the detailed structures of ten new materials based on the mononuclear zinc complexes of tetra(4-chlorophenyl) porphyrin and tetra(4-fluorophenyl)porphyrin in various stoichiometric combinations with molecular guest solvents (**1–7**, **9**, **10** and **12**), and ellucidate the typical interporphyrin aggregation modes and conditions of their occurrence. Crystal data for two additional solids with disordered and incompletely refined structures, **8** and **11**, are also indicated. The crystalline compounds referred to in this investigation are:

**1.** 2 : 1 Zn-4ClTPP : *o*-chlorotoluene [$2C_{44}H_{24}Cl_4N_4Zn \cdot C_7H_7Cl$];
**2.** 1 : 1 Zn-4ClTPP : guaiacol [$C_{44}H_{24}Cl_4N_4Zn \cdot C_7H_8O_2$];
**3.** 1 : 1 Zn-4ClTPP : nitrobenzene [$C_{44}H_{24}Cl_4N_4Zn \cdot C_6H_8NO_2$];
**4.** 1 : 2 Zn-4ClTPP : dimethylsulfoxide [$C_{44}H_{24}Cl_4N_4Zn \cdot 2C_2H_6OS$];
**5.** 1 : 2 Zn-4ClTPP : methyl salicylate [$C_{44}H_{24}Cl_4N_4Zn \cdot 2C_8H_8O_3$];
**6.** 1 : 2 Zn-4ClTPP : L-$\alpha$-methylbenzylamine [$C_{44}H_{24}Cl_4N_4Zn \cdot 2C_8H_{11}N$];
**7.** 1 : 1 Zn-4ClTPP : benzyl alcohol [$C_{44}H_{24}Cl_4N_4Zn \cdot C_7H_8O$];
**8.** 2 : 1 Zn-4ClTPP : *m*-dichlorobenzene [$2C_{44}H_{24}Cl_4N_4Zn \cdot C_6H_4Cl_2$];
**9.** 1 : 1 Zn-4FTPP : *p*-xylene [$C_{44}H_{24}F_4N_4Zn \cdot C_8H_{10}$];
**10.** 1 : 2 Zn-4FTPP : acetophenone [$C_{44}H_{24}F_4N_4Zn \cdot 2C_8H_8O$];

**11.** 1 : 2 Zn-4FTPP : anisole [$C_{44}H_{24}F_4N_4Zn \cdot 2C_7H_8O$];
**12.** Zn–4FTPP [$C_{44}H_{24}F_4N_4Zn$].

## 2. Experimental

Zn-tetra(4-chlorophenyl)porphyrin [Zn-4ClTPP] and Zn-tetra(4-fluorophenyl) porphyrin [Zn-4FTPP] were purchased from Midcentury Chemicals (Posen, Illinois); standard literature methods for the preparation of the porphyrin compounds are given in Ref. [25]. Their various complexes (see above) with other molecular species were obtained by recrystallization of the porphyrin derivative from a minimum amount of the respective liquid guest component. Crystals of the pure fluoro derivative were obtained from *o*-chlorophenol. Common solvents (such as methanol, glacial acetic acid, ethyl acetate) were used in some cases to control the solubility of the tetraphenylporphyrin derivative. Suitable crystals for X-ray diffraction were prepared in various ways, including slow cooling, solvent diffusion, and solvent evaporation in the open air for long periods of time (several weeks). Some of the crystals had to be covered by an epoxy resin to avoid their deterioration during the diffraction experiments.

The X-ray diffraction experiments were carried out at room temperature on an automated CAD4 diffractometer equipped with a graphite monochromator. Intensity data were collected by the $\omega$–$2\theta$ scan mode with a constant speed (either 2.0 or 4.0 deg/min, according to the diffraction power of the analysed crystal), using Mo-$K_\alpha$ radiation ($\lambda = 0.7107$ Å). Three standard reflections from different zones of the reciprocal space were measured periodically, with no significant variation. No corrections for absorption and secondary extinction effects were applied. The crystal data and pertinent details of the experimental conditions are summarized in Table I.

The crystal structures were solved by a combination of direct methods (SHELXS-86 [7]). Their refinements were carried out by either a full-matrix or large-block least-squares, including the positional and thermal parameters of the non-hydrogen atoms. The refinement calculations were based on $F^2$ (SHELXL-93, [8]). In order to maximize the data-to-parameters ratio the phenyl groups were characterized by a constrained geometry. The hydrogen atoms were introduced in calculated positions, the methyls being treated as rigid groups. In most cases, the refinements converged at reasonably low $R$-values (Table I), allowing a reliable description of the atomic parameters and of the intermolecular organization and interaction scheme. The final difference electron-density maps of the ten structures (all with peaks and troughs of $< 0.8\ e\ \text{Å}^{-3}$) showed no indication of incorrectly placed or missing atoms.

Some difficulties experienced in the refinement procedures, similar to those typically observed in related studies of composite porphyrin structures [3, 5, 9], are detailed below. The intensity distribution in the corresponding diffraction patterns

TABLE I. Summary of crystal data and experimental parameters for the fully analysed materials.

| Compound | **1** | **2** | **3** | **4** | **5** | **6** | **7** | **9** | **10** | **12** |
|---|---|---|---|---|---|---|---|---|---|---|
| $FW$[a] | 1758.4 | 940.1 | 939.0 | 972.2 | 1120.2 | 1058.3 | 924.0 | 856.2 | 990.4 | 750.1 |
| Space group | $P\bar{1}$ | $P\bar{1}$ | $P\bar{1}$ | $P\bar{1}$ | $P1$ | $P1$ | $Cc$ | $P\bar{1}$ | $P\bar{1}$ | $I2_12_12_1$ |
| $Z$ | 2 | 4 | 4 | 2 | 1 | 1 | 4 | 1 | 1 | 4 |
| $a$, Å | 9.219(5) | 16.722(2) | 16.729(3) | 10.774(2) | 8.942(2) | 11.031(1) | 17.215(2) | 7.705(1) | 8.309(2) | 13.984(2) |
| $b$, Å | 19.906(5) | 16.767(3) | 16.785(2) | 14.330(3) | 12.265(4) | 11.699(1) | 15.070(2) | 11.302(2) | 12.072(2) | 15.371(3) |
| $c$, Å | 22.478(4) | 18.500(3) | 18.231(8) | 16.647(4) | 12.755(2) | 12.787(2) | 18.744(7) | 12.446(5) | 12.895(3) | 15.383(4) |
| $\alpha$, deg | 84.47(2) | 66.94(2) | 72.08(2) | 67.83(2) | 80.86(2) | 115.45(1) | 90.0 | 90.39(2) | 76.50(2) | 90.0 |
| $\beta$, deg | 78.20(2) | 72.05(1) | 66.44(3) | 71.95(2) | 79.58(2) | 110.60(1) | 116.01(3) | 104.14(3) | 81.96(2) | 90.0 |
| $\gamma$, deg | 76.62(3) | 62.43(1) | 62.12(2) | 82.20(2) | 69.53(3) | 98.63(1) | 90.0 | 101.82(2) | 70.48(2) | 90.0 |
| $V$, Å$^3$ | 3923.0 | 4179.1 | 4101.5 | 2262.5 | 1282.0 | 1303.2 | 4370.2 | 1026.8 | 1182.7 | 3306.6 |
| $D_c$, g cm$^{-3}$ | 1.49 | 1.49 | 1.52 | 1.43 | 1.45 | 1.35 | 1.40 | 1.38 | 1.39 | 1.51 |
| $F(000)$ | 1788 | 1920 | 1912 | 996 | 574 | 546 | 1888 | 440 | 510 | 1528 |
| $\mu$, cm$^{-1}$ | 9.89 | 9.06 | 9.23 | 9.24 | 7.56 | 7.32 | 8.63 | 6.69 | 5.94 | 8.20 |
| $2\theta$ limits, deg | 42 | 42 | 42 | 50 | 50 | 50 | 50 | 50 | 50 | 50 |
| $N$ (unique) | 6923 | 7842 | 7704 | 6846 | 4141 | 4420 | 3722 | 3455 | 3924 | 2686 |
| $N$ (obs)[b] | 4247 | 5565 | 5555 | 4544 | 3346 | 3690 | 2982 | 3026 | 3309 | 2036 |
| $R_F$ | 0.075 | 0.064 | 0.059 | 0.077 | 0.054 | 0.058 | 0.051 | 0.050 | 0.058 | 0.072 |
| $\lvert\Delta\rho\rvert_{max}$ | 0.77 | 0.48 | 0.46 | 0.73 | 0.39 | 0.56 | 0.36 | 0.52 | 0.58 | 0.48 |

[a]Formula weights refer to the compositions defined in the text.

[b]$I > 2\sigma(I)$.

is determined primarily by the spatial arrangement of the large porphyrin moieties. The experimental data are often not sensitive enough to reliably detect incommensurate symmetries (if present) of the porphyrin and the much smaller solvent component. It is difficult, therefore, to assess whether the apparent disorder of the latter in a number of structures (see below) is genuine, or is an artifact resulting from the imposed space symmetry. In fact, a significant disorder of the smaller component incorporated into the Zn-4ClTPP lattice is characteristic of many of the structural models discussed in this study. In structure **1** molecules of the *o*-chlorotoluene solvent, not coordinated to the metalloporphyrin core, are located on, and disordered about, the crystallographic inversion centers in the interporphyrin space. In structure **2**, one of the uncoordinated guest guaiacol molecules is also structurally disordered between two sites. In structure **4** the DMSO guest species, which are ligated to the porphyrin metal ions through their oxygen site, exhibit a common configurational disorder characterized by the presence of two mirror-image structures of the $=S(CH_3)_2$ fragment. An interesting feature was observed also in structure **5**. Molecules of the methylsalicylate guest appear to ligate to the zinc ions in a randomly disordered manner, through their hydroxyl group at one site and through their carbonyl function (though more weakly) at another site. Each such ligand was, therefore, assumed to be present in the crystal in two different orientations; the relative occupancy factors of the latter was determined in the crystallographic refinement. The refinement calculations of this model converged well, but the apparent disorder of the methylsalicylate affected the precision of its atomic parameters. Structure **6**, which involves a 5-coordinate metalloporphyrin species with a chiral guest component ($\alpha$-methylbenzylamine), appeared to contain a significant amount of the *R*-isomer in addition to the L-isomer. This can be attributed to the fact that the commercial reagent used in crystallization was not fully resolved and optically pure. The crystallographic refinement indicated a disordered arrangement of the Zn ion below and above the porphyrin plane, with a distance of about 0.9 Å between the two sites, as well as a 'disordered' configuration of the *R*-$CH(CH_3)NH_2$ fragment (interchange between the H and $NH_2$ sites). The ratio between the two inverted configurations was refined to be approximately 82 : 18. These features resemble 'inversion twinning' about the porphyrin center, previously observed for another porphyrin structure [10]. Minor disorder of the *p*-xylene guest has also been observed in structure **9**. Some of the disordered guests referred to above were assigned isotropic temperature factors, and were refined with a constrained or restrained geometry, in order to avoid unreliable distortions of the covalent parameters.

Analysis of two additional compounds failed to provide rigorous results. A 2 : 1 complex of Zn-4ClTPP with *m*-dichlorobenzene (**8**) has been prepared and crystallized, but it could not be fully analysed due to the poor quality of the diffraction data and a significant guest disorder. Its crystals are triclinic with $a$ = 9.540(3), $b$ = 14.106(3), $c$ = 16.455(3) Å, $\alpha$ = 90.19(2), $\beta$ = 91.01(3), and $\gamma$ = 94.21(3)°, current $R$ = 0.104 for 2815 reflections above the intensity threshold

of $2\sigma(I)$. Similar difficulties were experienced with a 1 : 2 complex of Zn-4FTPP with anisole (**11**): monoclinic, space group $P2_1$, $a = 11.601(2)$, $b = 8.736(5)$, $c = 23.685(4)$ Å, $\beta = 91.78(1)°$. The refinement calculations of this structure converged poorly at $R = 0.14$ (for 2110 reflections above the intensity threshold) due to a major disorder of the anisole guest component. Crystals of both structures appeared to contain also molecules of water, but their exact composition could not be reliably determined, as crystallographic and thermal analyses provided inconsistent results. Still, the porphyrin organization in these structures appears to be reasonably well defined.

Lists of fractional coordinates and thermal parameters of the nonhydrogen atoms, atomic coordinates of the hydrogen atoms, as well as of bond lengths and bond angles for structures **1–12**, along with the atom labeling schemes used, have been deposited as supplementary material.

## 3. Results and Discussion

The molecular structures of the various metalloporphyrin molecules do not exhibit unusual features. Selected structural parameters involving the metal center and its coordination environment in the various compounds are summarized in Table II. All Zn—N(pyrrole) bond lengths cluster within 2.0–2.1 Å. In five-coordinate compounds the distances between the zinc ion and the coordinating atom are within 2.1–2.2 Å, while in the six-coordinate materials they are near 2.68 Å. In the square-planar and the square-bipyramidal arrangements the metal lies in the plane of the four pyrrole N-atoms; in the five-coordinate structures it deviates by 0.22–0.36 Å from this plane. Since the *intra*molecular parameters of these species have been subjected in the past to extensive experimental as well as theoretical investigations, and evaluated with great detail [1, 11], the following discussion will be devoted mostly to the description of the *inter*molecular features in the analysed materials.

### 3.1. STRUCTURES OF THE Zn(II)-TETRA(4-CHLOROPHENYL)PORPHYRINS

This group of compounds involves four-, five- and six-coordinate metalloporphyrin varieties. Experiments on the crystallization of Zn-4ClTPP from solvents lacking a strong Lewis base function leads to the formation of clathrates consisting of four-coordinate moieties. On the other hand, interaction with solvents containing either hydroxyl, carbonyl, or an amine function yields molecular complexes of five- and six-coordinate porphyrin entities. In the latter, the ligating component occupies the axial coordination sites of the metal center, above and below the porphyrin plane.

The most common motif of interporphyrin organization is revealed in structures **2–5**. In these solids, the large porphyrin frameworks form characteristic layers, within which the interporphyrin arrangement is characterized along one direction

TABLE II. Coordination parameters of the metal center in the various materials.

| Compound | Zn—N (porphyrin) bond length range (Å) | Zn coordination number, and type of axial ligands | Zn—axial ligand distance range (Å) | Zn deviation from the mean plane of the 4 N-atoms (Å) |
|---|---|---|---|---|
| **1** | 2.011–2.044(9) | 4 | – | 0.015, 0.022(4)[c] |
| **2** | 2.011–2.047(8) | 4 | – | 0.015, 0.035(2) |
| **3** | 2.008–2.041(7) | 4 | – | 0.006, 0.027(4) |
| **4** | 2.058–2.065(5) | 5, O=S | 2.123(9) | 0.322(2) |
| **5**[a] | 2.009–2.064(12) | 6, OH | 2.681–2.689(14) | 0.031(3) |
| **6**[b] | 2.048–2.100(9) | 5, $NH_2$ | 2.204(10) | 0.359(2) |
| **7** | 2.050–2.068(7) | 5, OH | 2.188(9) | 0.222(2) |
| **9** | 2.026–2.034(3) | 4 | – | 0.0 |
| **10** | 2.035–2.045(3) | 6, O=C | 2.682(3) | 0.0 |
| **12** | 2.021–2.031(6) | 4 | – | 0.0 |

[a]For guest orientation in which it coordinates to the metal center via the OH function.
[b]For the main component of the twinned structure.
[c]In compounds **1–3** there are two porphyrin molecules in the asymmetric unit.

by apparent Cl···Cl interactions between the *cis*-related chlorophenyl arms of adjacent moieties (see below). The interporphyrin cavity formed between the two Cl···Cl contacts is perfectly suited to a favorable occlusion of smaller molecular species. Intralayer packing along the other direction is stabilized by electrostatic attractions between opposing C—Cl dipoles. The observed architecture is further characterized by a tight steric fit between the convex Cl···Cl sites of one row of the porphyrins and the concave surface of an adjacent porphyrin row in a layer (Figure 1). This unique motif resembles the structural modes observed in the crystals of tetra-(4-hydroxyphenyl)porphyrin [4(OH)TPP] derivatives, in which assembly of the porphyrin building blocks is directed by hydrogen-bonding associations. Its occurrence suggests that the Cl···Cl interactions also play an important role in directing the intermolecular organization, irrespective of the type of stacking between parallel chains or layers of the porphyrin host. The most frequently observed structural motifs of the layered interporphyrin organization in the crystals based on 4ClTPP, 4(OH)TPP and unsubstituted TPP are illustrated in Figure 1.

Structures **2** and **3** are based on four-coordinate metalloporphyrin units and are nearly isomorphous; they are shown in Figures 2 and 3, respectively. In both structures the porphyrin layers are stacked in an offset manner. The interporphyrin cavities formed in each layer between the two pairs of the Cl···Cl contacts partly overlap, joining into a one-dimensional channel along a direction tilted about 30° away from the normal to the porphyrin layers. These channels are filled in the crystal by the guaiacol (in **2**) and nitrobenzene (in **3**) guest components. Packing along the stacking axis is stabilized mainly by dispersion forces, which are optimized by the offset stacked geometry of the overlapping porphyrin layers as well as by the

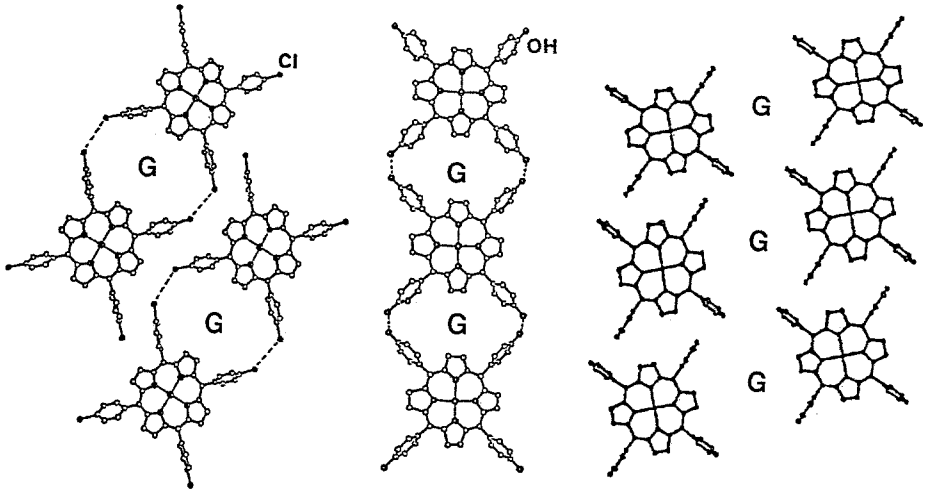


Fig. 1. Comparison of typical modes of the layered interporphyrin organization in crystals of (from left to right): (a) tetra(4-chlorophenyl)metalloporphyrin [5], (b) tetra(4-hydroxyphenyl)metalloporphyrin [5], and (c) tetraphenylmetalloporphyrin [4]. The label 'G' indicates sites of guest/solvent inclusion, representing either one or two small organic entities. The dashed lines in (a) and (b) represent Cl···Cl interactions and OH···OH hydrogen bonds, respectively. The interaction mode in (c) also involves T-shaped interactions between the phenyl rings of neighboring molecules, in which C—H bond dipoles of one group are oriented toward the negatively charged carbon atoms of an adjacent ring [24].

'saddle'-type conformation adopted by the porphyrin core [11]. The latter features characterize the sterically preferred arrangement of four-coordinate TPP units along the normal direction. Structure **3** represents one of the two known polymorphs of the Zn-4ClTPP clathrate with nitrobenzene. Another non-centrosymmetric polymorph of this compound has been characterized earlier; it represents a uniquely interesting example of a polar tubular interporphyrin lattice capable of aligning the dipolar guest molecule (nitrobenzene) in a given direction of the crystal bulk [5]. The two polymorphs were obtained from the same crystallization mixture. Semi-empirical calculations of packing energies, using the program OPEC [12] and suitably modified potential functions, have indicated only minor differences of 0.4–0.8 kJ $mol^{-1}$ between the two crystal structures.

Crystals of the five-coordinate complex of Zn-4ClTPP with DMSO (**4**) are composed of flat porphyrin networks of similar type as in the previous examples (Figure 4). These pair around the centers of the crystallographic inversion. The structure consists of 1 : 1 units of the DMSO-porphyrin complex. The DMSO ligand, bound through its carbonyl site to the metal center of one layer, at C=O···Zn of 2.123 Å, protrudes into the interporphyrin pores of an adjacent layer. The remaining empty space within these pores is occupied by a second non-coordinated molecule of the small DMSO guest. As in other five-coordinate metalloporphyrin structures, the Zn ion deviates (by 0.32 Å) from the plane of the planar porphyrin core, towards the bound ligand, assuming a square-pyramidal coordination geometry. The interlayer

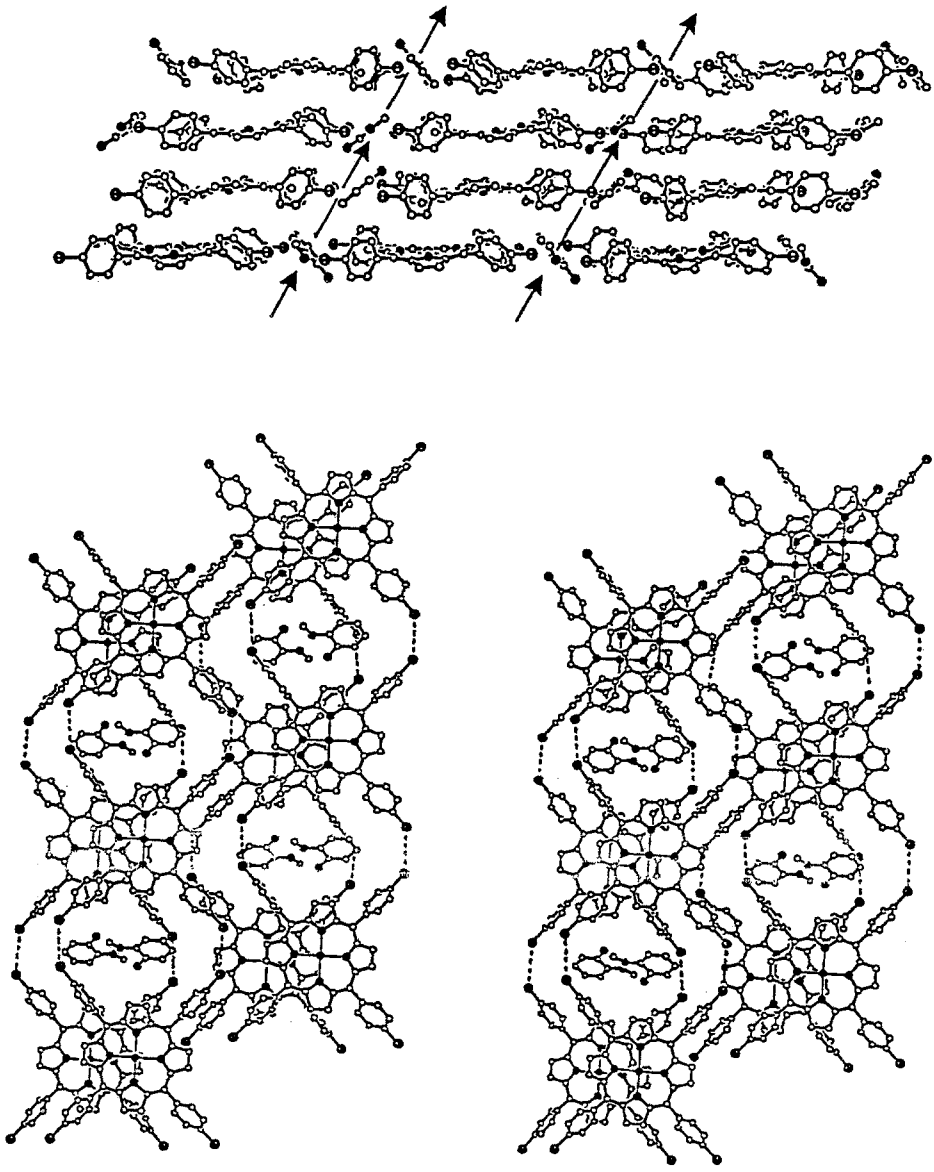

Fig. 2. (Bottom) Stereoview of the intermolecular architecture in **2**, showing occlusion of the guest entities within well defined interporphyrin pores. (Top) Edge-on view of the stacked layered arrangement of the Zn-4ClTPP building blocks. The arrows indicate the channel zones formed between the stacked porphyrin arrays in the lattice which are occupied by the guest solvent molecules.

packing in this structure is further optimized by an offset displacement of adjacent layers, so that some of the perpendicularly aligned phenyl rings of one layer point at the concave face of the five-coordinate porphyrin core of another layer.

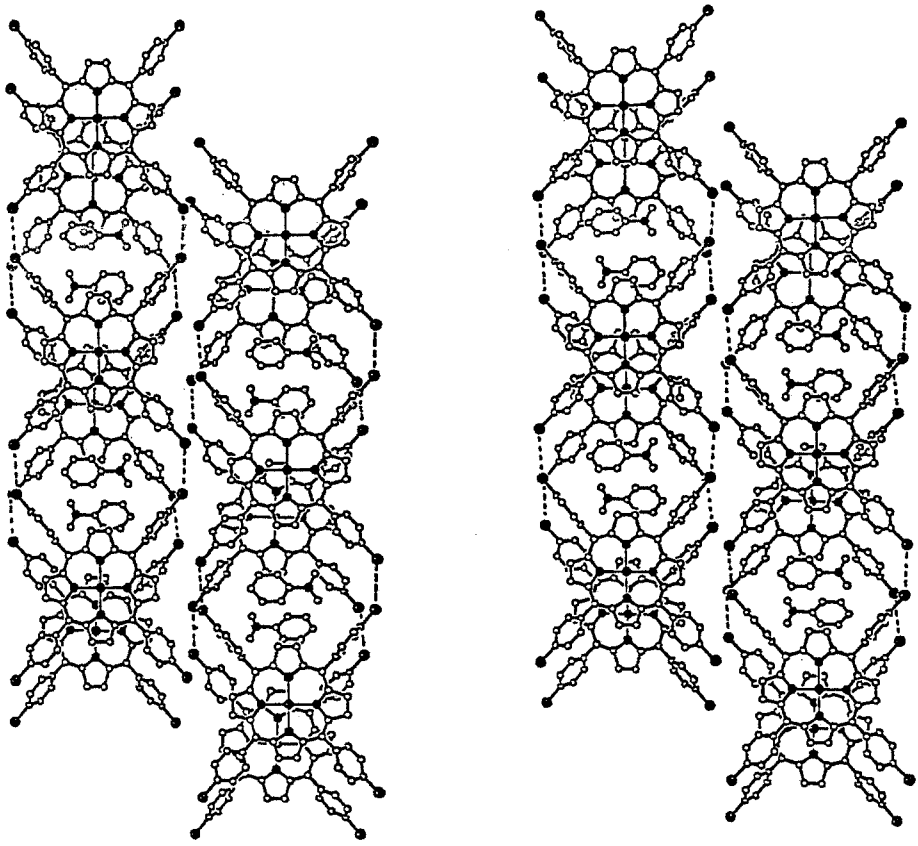

Fig. 3. Stereoview of the crystal structure of **3**, illustrating a typical intermolecular interaction scheme for the four-coordinate chloro-substituted porphyrin compounds.

Compound **5** contains two-dimensional porphyrin arrays very similar to the layered motif seen in structures **2–4**. In this compound, however, the lattice consists of six-coordinate metalloporphyrin complexes in which molecules of the salicylic methyl ester occupy the axial coordination sites. In the stacked arrangement of these layers the two metal ligating species of one unit of the complex protrude into, and effectively fill, the interporphyrin voids of the neighboring layers located above and below. The observed structure of the 1 : 2 complex is significantly disordered. The bifunctional ligands can interact with the zinc ion either through the carbonyl oxygen site, or through the hydroxyl group. The latter seem to be preferred, as indicated by somewhat shorter distances of coordination at Zn· · ·OH = 2.68 and 2.69 Å. Accordingly, a twofold disorder of these species was assumed in the refinement of the structural model to account for this phenomenon. Figure 5 illustrates the typical layered porphyrin arrangements, and the two possible

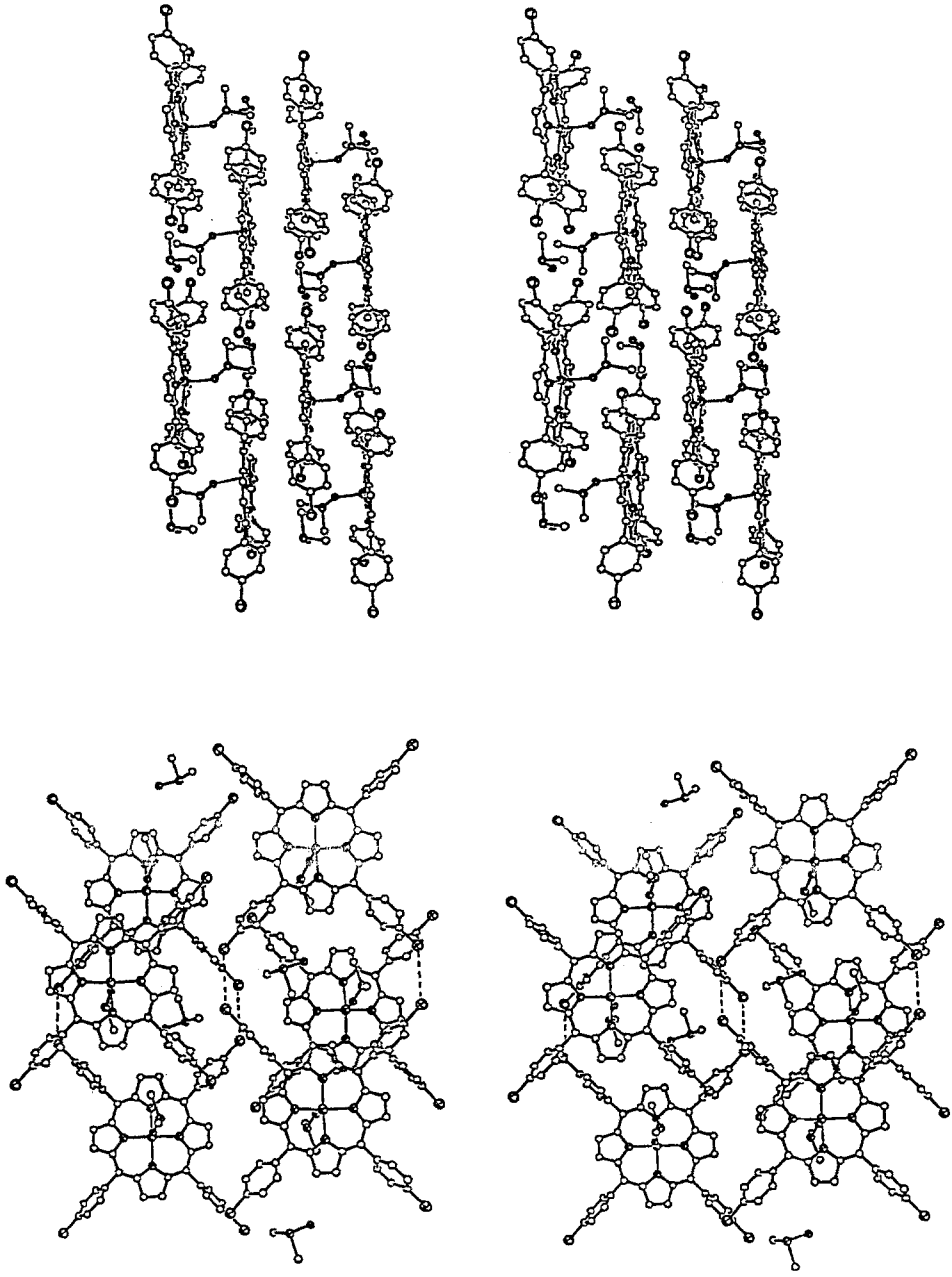

Fig. 4. Illustration of the crystal structure of **4**, involving five-coordinate metalloporphyrin moieties with the DMSO ligand. The two stereoviews show edge-on (top) and face-on (bottom) perspectives of the intermolecular organization. Both, the metal-coordinated as well as the uncoordinated ligand molecules occluded within the layers between the porphyrin units are shown.

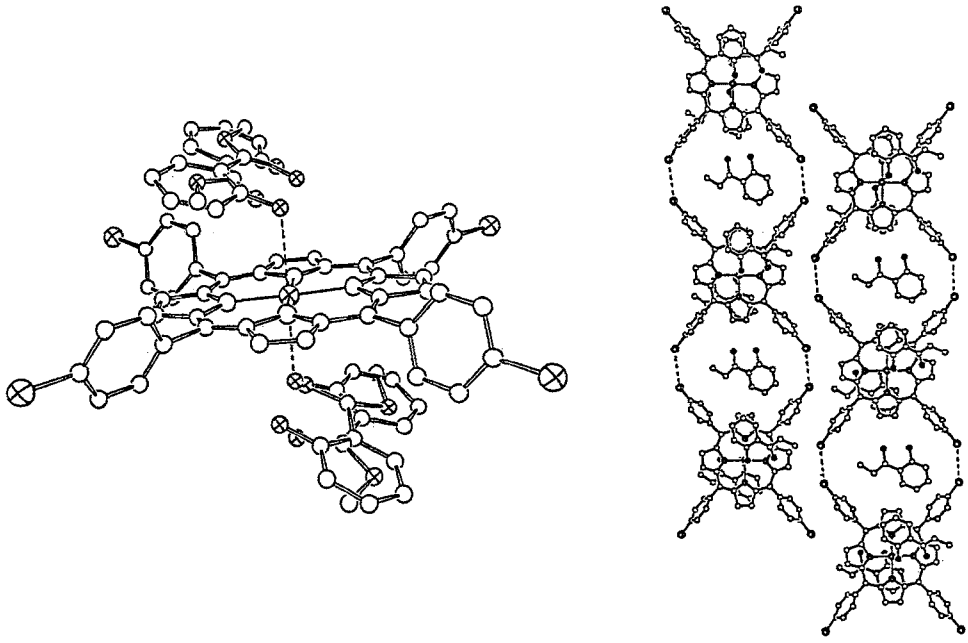

Fig. 5. The 1 : 2 complex of Zn-4ClTPP with methylsalicylate, **5**. (a: left) Illustration of a single six-coordinate entity, showing the twofold disorder of the axial ligands. Noticeably, in both orientations the latter occupy nearly the same volume above and below the porphyrin core. (b: right) A perspective view of the intermolecular arrangement. It includes six six-coordinate porphyrin units of one layer, and four guest molecules enclosed within the interporphyrin voids which ligate to metalloporphyrin cores of adjacent layers. For clarity, the ligands in (b) are shown only in one orientation.

positions and orientations of the ligands within the available space above and below the porphyrin core.

The average Cl···Cl nonbonding distances between the *cis*-related chlorophenyl arms of adjacent porphyrin moieties in the above structures are: 3.63 Å in **2**, 3.65 Å in **3**, 3.90 Å in **4** and 3.81 Å in **5**. The C—Cl bonds involved in these interactions approach one another roughly at right angles. These values lie well in the range of Cl···Cl distances which are indicative of specific interaction [13, 14]. The characteristic geometric patterns with small interporphyrin pores observed for **2–5** between the interacting Cl atoms, as well as for five other complexes of 4ClTPP reported earlier [5], is similar to the basic structural 'chain' motif found in the hydrogen-bonded chains of 4(OH)TPP derivatives, but is considerably different from that observed in crystals of the unsubstituted TPP compounds (Figure 1a–c) [4, 5]. Their common and dominant appearance in the 4ClTPP materials reflects on the importance of these interactions in the crystal structures referred to above.

The remaining four structures **1** and **6–8** represent different and less common modes of crystalline organization of the Zn-4ClTPP moieties. In compound **6** the packing of the porphyrin molecules resembles that found most frequently in the

lattice clathrates of unsubstituted TPP building blocks. The structure can be best described as consisting of chains of tightly packed porphyrins, with a nearly perpendicular arrangement of interacting chlorophenyl groups [C—Cl to $\pi$(aryl)] of adjacent molecules (Figure 6). These chains are stacked stepwise in corrugated sheets. The solvent molecules incorporated into the lattice are accommodated in channel-type zones which run parallel to the porphyrin planes and are bounded by four chains of porphyrin molecules. Along the channels they also occupy the axial coordination sites of the metalloporphyrin entity. However, in this case the chiral nature of the solvate involved, L-$\alpha$-methylbenzylamine as the major component (see Experimental), prevents formation of a symmetric six-coordinate complex containing an inversion center at the metal ion. In fact, careful evaluation of the experimental data indicates clearly that the basic unit in this compound is a 1 : 1 five-coordinate porphyrin–solvate entity. The zinc ion deviates by 0.36 Å from the porphyrin plane towards one of the surrounding ligands, and binds to its amine group at Zn· · ·$NH_2$ = 2.204 Å. The second molecule of the solvent approaches the concave side of the porphyrin core, with its $C_{(sp^3)}$—H bond directed towards the porphyrin, filling the empty space in this region. The optimally refined structural model derived from the diffraction data indicates that in the analysed crystal about 82% of the five-coordinate units of the complex are oriented in one direction, and about 18% exhibit an inverted structure (involving the *R*-isomer of the guest molecule) and point the other way. These observations beautifully reflect on the general tendency of the TPP materials to form centrosymmetric or pseudo-centrosymmetric intermolecular arrangements, and demonstrate the dominant effect of molecular shape on the supramolecular organization, particularly in the absence of specific directional forces between the porphyrin units.

Side-packing of the porphyrin chains is considerably tighter in compound **7**, while preserving the T-shaped interaction mode between the chlorophenyl rings of neighboring molecules within the chain. This structure is composed of a five-coordinate metalloporphyrin complex unit. It can be also described as containing layers of coplanar porphyrin molecules with localized cavities occupied by the coordinated ligands. All layers in the crystal are oriented in the same direction. Their stacking is such that the metal-coordinated benzyl alcohol ligand (at Zn· · ·OH = 2.188 Å) of one layer is inserted into the interporphyrin pores of another layer. This key-to-lock type steric complementarity yields an effectively packed crystal structure shown in Figure 7.

Figure 8 shows the intermolecular organization in compound **1**, and represents a 'herring-bone' type clathrate of four-coordinate 4ClTPP entity. This type of arrangement was previously observed in a small number of TPP lattice clathrates [4]. The structure is composed of stacks of the porphyrin molecules with the guest *o*-chlorotoluene solvent trapped in between. All stacks extend along the same axis, but the molecular planes in adjacent stacks are tilted in opposite directions with respect to the stack axis by about +30° or −30°. The incorporated solvent molecules are located on, and disordered about, the centers of crystallographic inversion. As

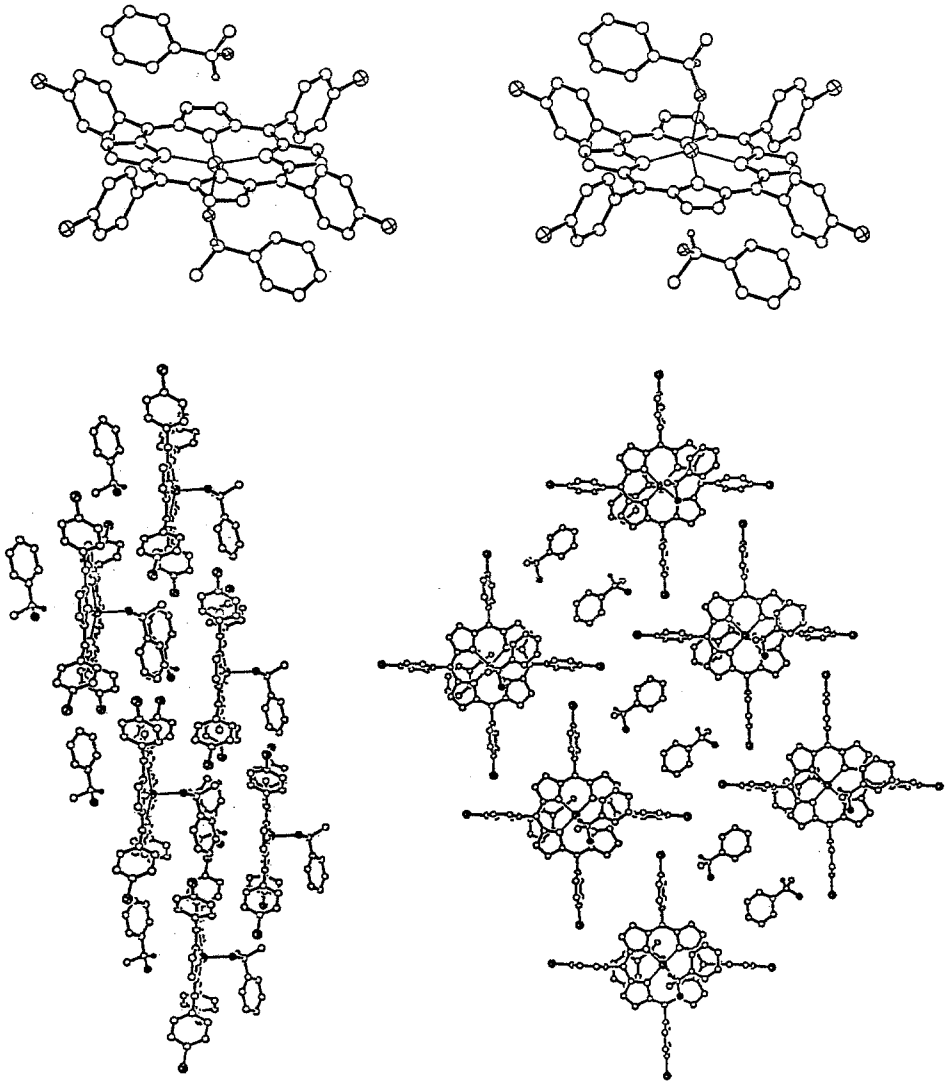

Fig. 6. The complex of Zn-4ClTPP with α-methylbenzylamine **6** (stoichiometric ratio 1:2). The two inverted entities (a five-coordinate complex and a non-coordinated guest molecule), shown at the top, are present in the crystal in a 82:18 ratio. Two perpendicular views of the overall intermolecular organization are illustrated at the bottom; for clarity only one configuration is shown. Note the T-shaped interactions between the chlorophenyl rings of adjacent molecules (C—Cl $\cdots$ $\pi$), and the intercalated arrangement of the guest components between corrugated sheets of the porphyrin frameworks (see Ref. [4]).

in the previous cases, stacking-type aggregation of the four-coordinate 4ClTPP moieties involves a considerable displacement of adjacent units from a complete overlap. It is also associated with a significant deformation from planarity of the porphyrin core (which assumes usually the 'saddle'-type form [11]), due to a

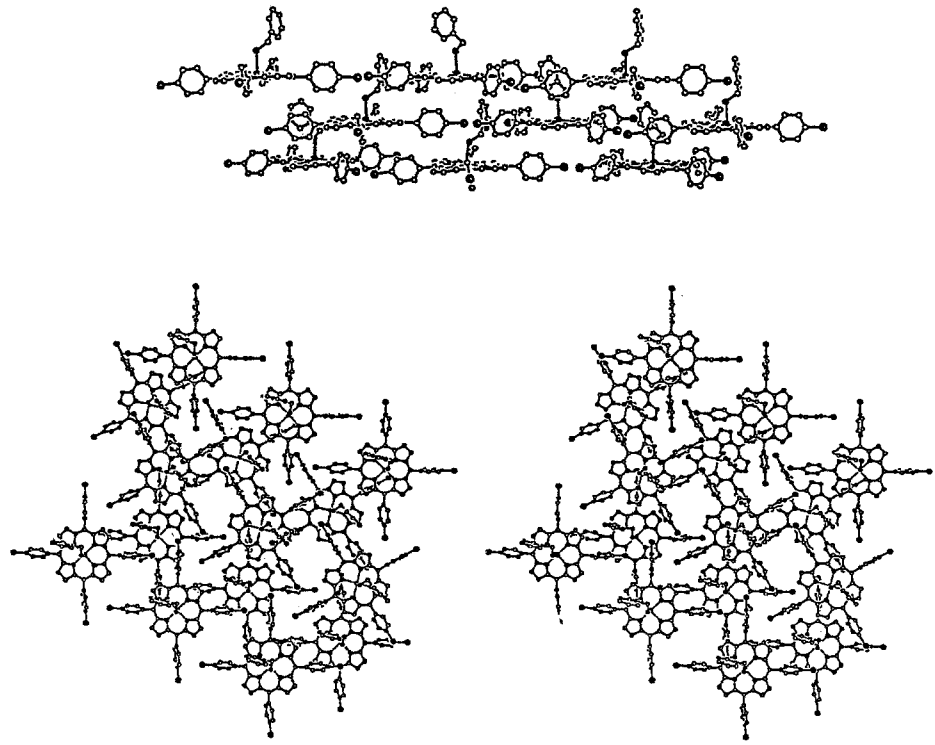

Fig. 7. (Bottom) The intermolecular architecture in structure **7**, stereoviewed down the normal to the porphyrin plane. (Top) An edge-on view of the crystal structure, showing the effective key-to-lock type steric complementarity between subsequent layers of the five-coordinate entities.

severe steric hindrance between the aryl substituents on the porphyrin core of the overlapping moieties.

The porphyrin lattice in compound **8** resembles to a significant extent that observed in **6** and in 'normal' triclinic tetraphenylporphyrin-based clathrates [4]. It contains condensed chain motifs which are characterized by an antiparallel arrangement of the polarized chlorophenyl groups (Figure 9a). The *m*-dichlorobenzene guest is accommodated in localized cavities surrounded by the chlorophenyl groups of four adjacent porphyrins.

### 3.2. STRUCTURES OF THE Zn(II)-TETRA(4-FLUOROPHENYL)PORPHYRINS

Solid complexes based on the fluorophenyl-substituted porphyrin building blocks crystallize with a greater difficulty than the corresponding chloro-derivatives. This observation can be attributed primarily to the different nature of nonbonding interactions between the peripheral groups [14, 15]. Direct F···F intermolecular contacts involve 'hard' end atoms, and are mostly of a repulsive nature. On the other hand, the Cl···Cl nonbonding interaction between the 'softer' chlorine atoms with an

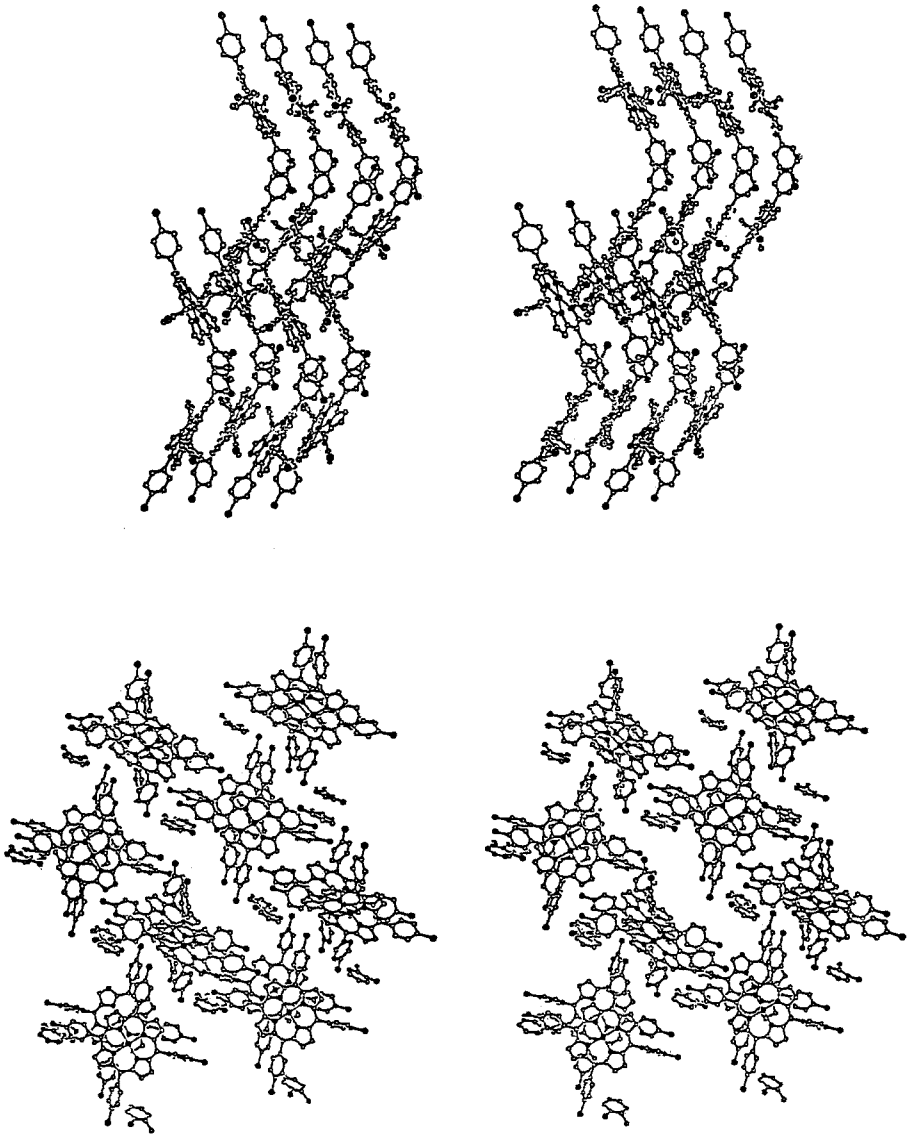

Fig. 8. Two stereoviews of the 'herring-bone' type structure of compound **1**. It consists of porphyrin stacks composed of four-coordinate entities, with molecules of the *o*-chlorotoluene solvent incorporated in between.

appropriate directional geometry provides an attractive contribution to the lattice stabilization energy. Within the framework of the current study we were able to obtain good quality crystals of the solvent free compound Zn(II)-4FTPP, as well as of a small number of its clathrates and complexes with different guests. It is important to note in this context that sizeable solvent free crystals of either M-4ClTPP or M-4(OH)TPP materials could not be obtained thus far. This is most

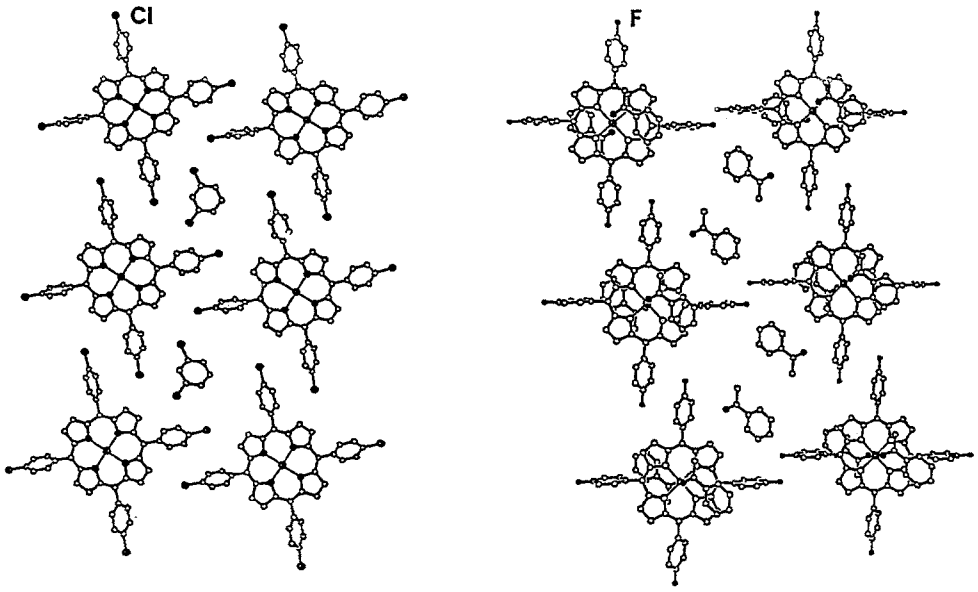


Fig. 9. Illustration of the intermolecular organization (single layer) in (a: left) clathrate **8** based on four-coordinate Zn-4ClTPP entities, and (b: right) the structure of the six-coordinate complex **10** based on Zn-4FTPP units. The porphyrin packing patterns in the two solids are similar to those observed in 'normal' and 'expanded' clathrates of unsubstituted tetraphenylporphyrins [4]. The four molecules of acetophenone enclosed between the shown porphyrin units in (b) are coordinated in the crystal to the metal centers of adjacent porphyrin layers approaching from above and below.

probably due to the different interaction potential associated with the —Cl, —OH and —F peripheral substituents, as optimization of specific attractions between the polar sensor groups stabilizes the 'hollow' interporphyrin patterns.

The above argument is best represented by the structural parameters of clathrate **9**. This solid is the only known example based on the Zn-4FTPP units in which the overall pattern of the interporphyrin organization resembles that most frequently observed for the Zn-4ClTPP materials (Figure 10). As in compounds **2–5**, the porphyrin molecules are arranged in offset-stacked layers. The interporphyrin voids within each layer are considerably larger in this structure than in the corresponding chloro-substituted compounds due to the repulsive nature of the C— F· · ·F—C interactions between the two pairs of the *cis*-related fluorophenyl arms of neighboring molecules. The direct F· · ·F nonbonding contacts between adjacent molecules which surround the guest component in **9** are 4.1 and 4.2 Å (Figure 10), as compared to the range of 3.6–3.8 Å for the corresponding Cl· · ·Cl contacts observed in structures **2–5**. This is quite a dramatic difference, considering that van der Waals radii of covalently bound F and Cl atoms are 1.35 and 1.8 Å, respectively [16]. Along the other direction of every layer, adjacent porphyrin molecules are arranged more effectively, with an antiparallel orientation of the fluorophenyl dipoles at an average distance of about 3.4 Å between the planes. The latter indicates that dipolar forces

are important in stabilizing the observed architecture of this structure. The guest *p*-xylene molecules within the large interporphyrin voids exhibit minor orientational disorder around the inversion centers at 0, 0.5, 0. Although their positions are close to the axial coordination sites above and below the metalloporphyrin framework, the *p*-xylene species interact only weakly with the latter, the porphyrins being thus best described as four-coordinate moieties. This crystal structure is characterized by a low packing density and is relatively unstable.

Compound **10** represents a six-coordinate structure with an ideally centrosymmetric square-bipyramidal coordination environment around the metal center of the porphyrin entity (Figure 9b). The ligating distances to the central ion are Zn···N (porphyrin) 2.035 and 2.045 Å, and Zn···O=C(solvate) = 2.682 Å, the latter representing weak interaction. The interporphyrin organization in **10** is an 'expanded' version of that observed in structure **6**. The porphyrin chains in this structure exhibit an antiparallel arrangement of nearest-neighbor fluorophenyl groups which optimizes dipolar association, but lacks the perpendicular C—Cl to phenyl interactions between adjacent molecules due to a strongly repulsive nature of such interactions with the 'hard' fluorine atoms. Due to the expanded structure of these chains, their coplanar aggregation is associated with the creation of large in-plane interporphyrin voids. The acetophenone ligands approaching from above and below from adjacent layers are fully encapsulated in pairs in the latter. This allows an effective interlayer approach and a tight packing in a direction perpendicular to the porphyrin planes.

In the monoclinic crystal structure of the anisole complex **11** the sheet structure of the porphyrin entities is disrupted by the screw symmetry axis operation, yielding instead a 'herring-bone' type array of the porphyrin chains. Lacking a strong polar functionality, the anisole species are not coordinated to the metal centers, and exhibit a considerable structural disorder in the interphase channels between adjacent chains. Similar motifs of 'expanded' and 'herring-bone' porphyrin patterns have also been observed in a number of lattice clathrates of the unsubstituted tetraphenylmetalloporphyrins [4].

The solvent-free structure of four-coordinate Zn(II)-4FTPP units, **12**, is illustrated in Figure 11. It consists of layers of the porphyrin molecules which are stacked one on top of the other in an offset manner. In the offset stacked geometry each porphyrin core is sandwiched between two pairs of antiparallel fluorophenyl arms of adjacent molecules from the layers above and below. Each such pair of the substituted aryl groups makes an edge-on approach to a metalloporphyrin core of the upper layer and at the same time protrudes into the empty interporphyrin space in the lower layer. Optimization of the crystal packing in this structure is thus associated with a significant ruffling/distortion from planarity of the porphyrin core, due to the sterically asymmetric environment around the individual molecules.

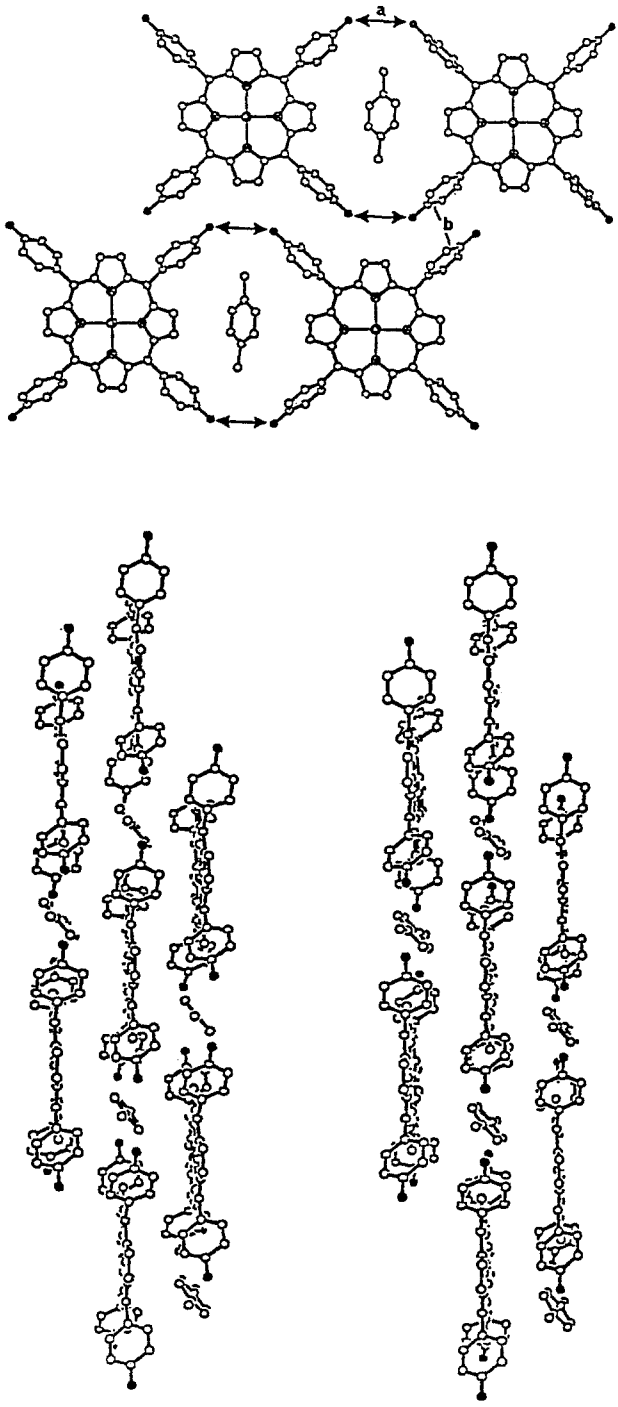


Fig. 10. Illustration of the crystal structure of clathrate **9**: (a: top) a single molecular layer, and (b: bottom) a stereoview of the overall packing. The layered arrangement of the metalloporphyrin molecules shown in (a) is similar to that observed in the Zn-4ClTPP materials **2–5**. However, the direct F···F contacts between adjacent porphyrins 'a' (marked by dark arrows), are rather larger (4.1–4.2 Å), reflecting the repulsive nature of these interactions. The average distance between the dipolarly interacting fluorophenyl groups 'b' is 3.4 Å.

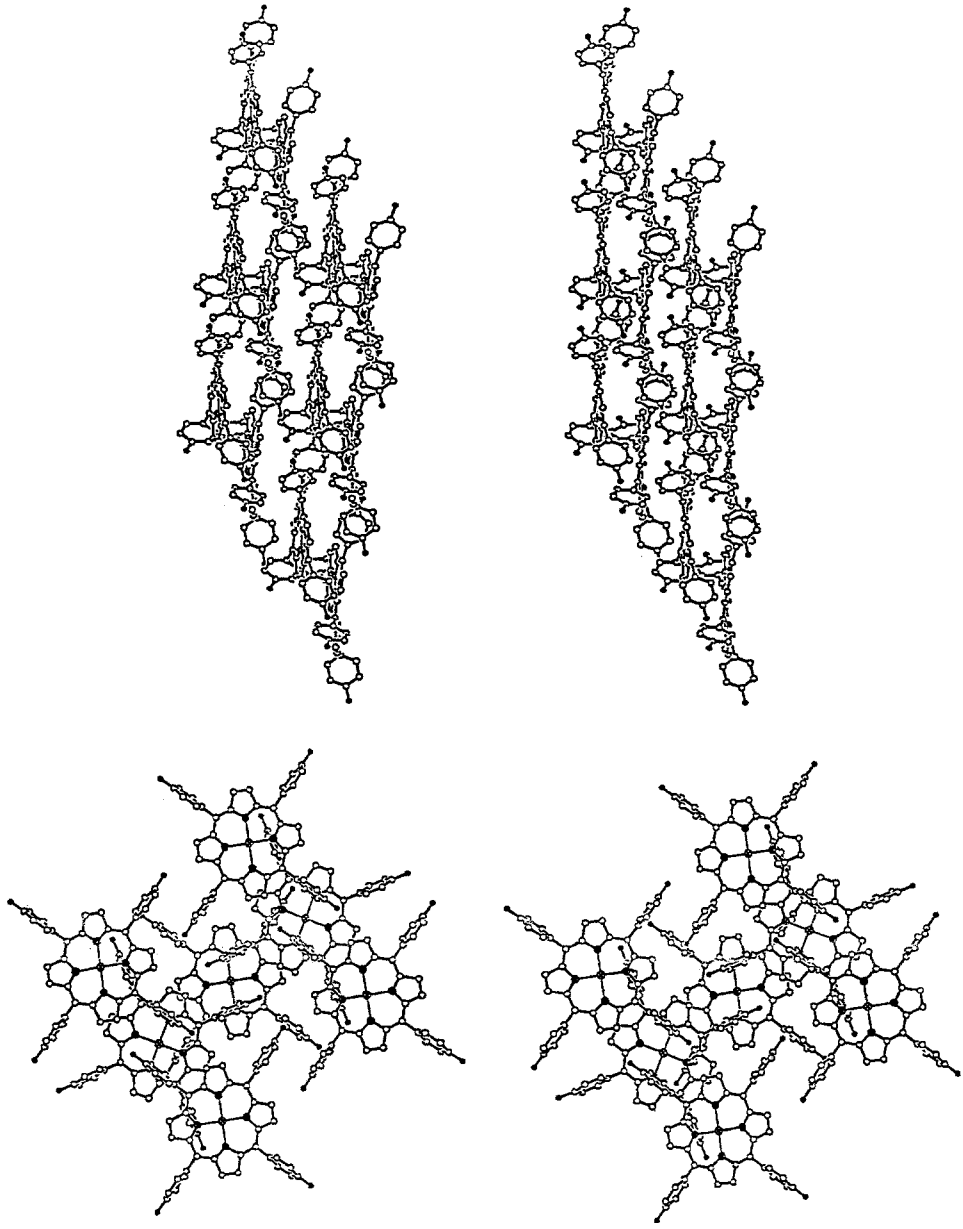

Fig. 11. Two stereoviews of the crystal structure of Zn-4FTPP. Note the severe ruffling of the metalloporphyrin cores and deformation of the porphyrin layers in order to optimize a condensed intermolecular aggregation in the absence of guest moieties.

## 4. Concluding Remarks

Dipolar forces and weak Cl···Cl interactions add to dispersion (molecular shape) effects in directing the intermolecular architecture of the halogen-substituted M-

TPP materials. The experimental difficulties to obtain large crystalline aggregates based on the Zn-4FTPP compound, along with the available results, indicate that the fluorophenyl groups contribute unfavorably to the lattice stabilization. In the absence of specific directional binding interactions between the peripheral functions, the dominant effect of the molecular shape on crystalline packing is similar for these compounds and the unsubstituted TPP derivatives. On the other hand, halogen–halogen interactions appear to be important in the chloro-substituted compounds. The most common motif of intermolecular architecture in the latter is a chain-type arrangement in which the porphyrin frameworks interact through the *cis*-related chlorophenyl residues of neighboring moieties, thus creating interporphyrin enclosures sufficiently large to effectively occlude molecules of small organics. This mode of supramolecular organization has been observed in about 75% of the known structures of the Zn-4ClTPP materials. The control of crystalline arrangements by weak interactions of the Cl· · ·Cl and OH· · ·OH type, demonstrated in this and the preceding studies [Figure 1a,b; Refs. 5 and 17], has been found to be important in the design of nonlinear optical materials [18, 19], solid- state reactive materials [13, 14, 19–21], and self-assembling systems [22, 23].

The supramolecular hollow architectures of the functionalized-porphyrin materials, and their inclusion behaviour, to some extent resemble characteristic features of inorganic microporous solids utilized in storage and transport of molecules and ions. Several types of crystalline aggregates in which the porphyrin organization in pseudorigid two-dimensional and three-dimensional arrays is affected by directional hydrogen bonding [5, 17], metal–ligand coordination [6] and Cl· · ·Cl interactions [5] have been prepared and identified thus far, and more than 50 new materials of the three types have been structurally defined. Further characterization of thermodynamic stability and guest release and exchange dynamics of such systems both in crystalline and polycrystalline forms, an important prerequisite for revealing structure–property relationships in these materials, is currently in progress.

## Acknowledgement

This research was supported in part by grant No. 90-00061 from the United States–Israel Binational Science Foundation (BSF), Jerusalem, Israel.

## References

1. W.R. Scheidt and Y.J. Lee: *Struct. Bond. (Berlin)* **64**, 1 (1987), and references cited therein.
2. M.P. Byrn, C.J. Curtis, S.I. Khan, P.A. Sawin, R. Tsurumi and C.E. Strouse: *J. Am. Chem. Soc.* **112**, 1865 (1990).
3. M.P. Byrn, C.J. Curtis, I. Goldberg, Y. Hsiou, S.I. Khan, P.A. Sawin, S.K. Tendick and C.E. Strouse: *J. Am. Chem. Soc.* **113**, 6549 (1991).
4. M.P. Byrn, C.J. Curtis, Y. Hsiou, S.I. Khan, P.A. Sawin, S.K. Tendick, A. Terzis and C.E. Strouse: *J. Am. Chem. Soc.* **115**, 9480 (1993).
5. I. Goldberg, H. Krupitsky, Z. Stein, Y. Hsiou and C.E. Strouse: *Supramol. Chem.* **4**(3) (1995) in press.
6. H. Krupitsky, Z. Stein, I. Goldberg and C.E. Strouse: *J. Incl. Phenom.* **18**, 177 (1994).

7. G.M. Sheldrick, SHELXS-86, in *Crystallographic Computing 3*, eds. G.M. Sheldrick, C. Kruger and R. Goddard, Oxford University Press, pp. 175–189 (1985).
8. G.M. Seldrick, SHELXL-93, *Program for the Refinement of Crystal Structures from Diffraction Data*, University of Goettingen, Germany (1993).
9. A.G. Golder, K.B. Nolan, D.C. Povey and L.R. Milgram: *Acta Crystallogr., Section C* **44**, 1916 (1988).
10. M.P. Byrn and C.E. Strouse: *J. Am. Chem. Soc.* **113**, 2501 (1991).
11. O.Q. Munro, J.C. Bradley, R.D. Hancock, H.M. Marques, F. Marsicano and P.W. Wade: *J. Am. Chem. Soc.* **114**, 7218 (1992).
12. A. Gavezzotti: *J. Am. Chem. Soc.* **105**, 5220 (1983) and **111**, 1835 (1989).
13. G.R. Desiraju: in *Organic Solid State Chemistry*, Ed. G.R. Desiraju, Elsevier, Amsterdam, Ch. 14 pp. 519–546 (1987).
14. G.R. Desiraju: in *Crystal Engineering – The Design of Organic Solids*, Ed. G.R. Desiraju, Elsevier, Amsterdam (1989).
15. E. Weber, N. Dorpinghaus, C. Wimmer, Z. Stein, H. Krupitsky and I. Goldberg: *J. Org. Chem.* **57**, 6825 (1992).
16. L. Pauling: *The Nature of the Chemical Bond*, 3rd Ed., Cornell University Press, Ithaca, NY (1960).
17. I. Goldberg, H. Krupitsky and C.E. Strouse: XVI Congress of the International Union of Crystallography, Beijing, China (1993). *Acta Crystallogr. Section A* **49** (Suppl.), C166 (1993).
18. D. Chemla and J. Zyss (Eds.): *Nonlinear Optical Properties of Organic Molecules and Crystals*, Academic Press, New York, Volumes 1 and 2 (1987).
19. M.C. Etter: *J. Phys. Chem.* **95**, 4601 (1991).
20. V. Ramamurthy (Ed.): *Photochemistry in Organized and Constrained Media*, VCH-Verlagsgesellschaft, Weinheim (1991).
21. R. Bishop, D.C. Craig, I.G. Dance, S. Kim, M.A.I. Mallick, K.C. Pich and M.L. Scudder: *Supramol. Chem.* **1**, 171 (1993).
22. P. Tecilla, R.P. Dixon, G. Slobodkin, D.S. Alavi, D.H. Waldeck and A.D. Hamilton: *J. Am. Chem. Soc.* **112**, 9408 (1990).
23. M. Hagihara, N.J. Anthony, T.J. Stout, J. Clardy and S.L. Schreiber: *J. Am. Chem. Soc.* **114**, 6568 (1992).
24. G. Klebe and F. Diederich: *Phil. Trans. Roy. Soc. London. A.* **345**, 37 (1993), and references cited therein.
25. A.D. Adler, F.R. Longo, J.D. Finarelli, J. Goldmacher, J. Assour and L. Korsalioff: *J. Org. Chem.* **32**, 476 (1967).